Polariton Theory of Resonance Raman Scattering in Insulating Crystals*

BERNARD BENDOW† AND JOSEPH L. BIRMAN‡
Physics Department, New York University, New York, New York 10453
(Received 15 August 1969)

A multibranch polariton theory of Raman scattering in insulators is presented; actual calculations of the resonance cross section are carried out for an undamped two-branch model, for various values of photon-exciton coupling and background dielectric constant, including values appropriate to CdS. One obtains a double peaking with incoming photon frequency, corresponding to the experimentally observed in- and outgoing photon resonances. Comparison with bare- and generalized-exciton computations shows that the results of the three theories are nearly the same for "smaller" couplings, as in CdS, except in the immediate region of the higher-energy peak; as the coupling increases from values near those in CdS, the predictions of the three theories begin to differ more substantially. When the exciton continuum is included by perturbation theory, the nearly similar predictions of the polariton and exciton theories, for frequencies below the bare-exciton frequency, are in agreement with experimental data on LO-phonon Raman scattering in CdS.

I. INTRODUCTION: FUNDAMENTALS OF POLARITON THEORY

POLARITONS are composite quasiparticles formed in an insulating crystal, for example, by the coupling of the exciton, phonon, and electromagnetic fields. A number of treatments of a variety of light-scattering problems, from a polariton point of view, have appeared in the literature,[1–4] since Huang's pioneer treatment of the classical photon-lattice case[5] and Fano's quantum-mechanical treatment.[6]

Recent experiments on Raman scattering (RS) in insulators such as CdS[7,8] have led to increased interest in the threoetical treatment of resonance RS. Ganguly and Birman[9] have presented a bare-exciton theory of RS, and the present authors have elsewhere generalized this approach to include a dispersive index of refraction and to incorporate damping from a first-principles calculation.[10] The latter approach leads to well-defined cross sections throughout the resonance region.

A number of treatments of RS from the polariton point of view have also recently been advanced.[11] However, actual calculations of the cross sections have not been made; also, we believe certain of the problems encountered in performing actual calculations have not been sufficiently emphasized. Here we present a treatment leading to an actual two-branch polariton calculation, while emphasizing certain of the steps in evaluating polariton cross sections. Calculations are carried out for a variety of cases, including parameters appropriate to CdS. Such calculations are especially useful in critically evaluating the implications of a number of authors[11] that the use of polariton theory is mandatory for couplings of the order of those in CdS.

We now present a brief review of certain relevant aspects of polariton theory.

Assume one has a bilinear interaction Hamiltonian[12]

$$\bar{H}=\Sigma_{\mathbf{k}}\bar{H}(\mathbf{k}),$$

$$\bar{H}(\mathbf{k})=\sum_{\lambda,\lambda'=1}^{n}[d_{\lambda\lambda'}a_{\lambda\mathbf{k}}{}^{+}a_{\lambda'\mathbf{k}}{}^{-}+(g_{\lambda\lambda'}a_{\lambda\mathbf{k}}{}^{+}a_{\lambda'-\mathbf{k}}{}^{+}+\text{Hermitian conjugate})], \quad (1.1)$$

where $D^{\dagger}=D$, $G=\tilde{G}$, and the $a^{\pm}$'s are boson operators of the free photon, exciton, and phonon fields, say. If the interactions are small enough to insure the stability of the system, then the eigenvalues of the $2n\times 2n$ matrix $M(\mathbf{k})$,

$$M\equiv\begin{pmatrix} D & G \\ -G^{*} & -D^{*}\end{pmatrix}, \quad (1.2)$$

are $(\pm)$ the n real polariton frequencies $\omega(\mathbf{k}\gamma)$. The matrix C formed from the eigenvectors of M defines the linear transformation to the polariton operators $A_{\mathbf{k}}{}^{\pm}$,

$$\begin{pmatrix} A_{\lambda\mathbf{k}}{}^{-} \\ A_{\lambda,-\mathbf{k}}{}^{+}\end{pmatrix}=C\begin{pmatrix} a_{\lambda\mathbf{k}}{}^{-} \\ a_{\lambda,-\mathbf{k}}{}^{+}\end{pmatrix}, \quad (1.3)$$

* Supported in part by U. S. Army Research Office (Durham) and the Aerospace Research Laboratories, Wright-Patterson Air Force Base (Dayton).

† Work based in part on a Ph.D. thesis submitted to New York University by B. Bendow, 1969. Present address: Physics Department, University of California, San Diego, La Jolla, Calif.

‡ Present address: Groupe de Physique des Solides, de l'E. N. S., and Laboretoire de Physique des Solides, Faculté des Sciences, Université de Paris, Paris 5, France.

[1] J. J. Hopfield, Phys. Rev. **112**, 1555 (1958); V. M. Agranovich, Zh. Eksperim. i Teor. Fiz. **37**, 430 (1959) [English transl.: Soviet Phys.—JETP **10**, 207 (1960)].

[2] L. N. Ovander, Usp. Fiz. Nauk **86**, 3 (1965) [English transl.: Soviet Phys.—Usp. **8**, 337 (1965)], and references listed therein.

[3] C. Mavroyannis, J. Math. Phys. **8**, 1515 (1967); **8**, 1522 (1967).

[4] W. C. Tait and R. L. Weither, Phys. Rev. **178**, 1404 (1969).

[5] K. Hunang, Nature **167**, 779 (1951); Proc. Roy. Soc. (London) **A208**, 352 (1951).

[6] U. Fano, Phys. Rev. **103**, 1202 (1956).

[7] R. C. C. Leite and S. P. S. Porto, Phys. Rev. Letters **17**, 10 (1966).

[8] R. C. C. Leite and J. F. Scott, in *Light Scattering Spectra of Solids*, edited by G. B. Wright (Springer-Verlag, New York, 1969).

[9] A. K. Ganguly and J. L. Birman, Phys. Rev. **162**, 806 (1967).

[10] B. Bendow and J. L. Birman (to be published).

[11] E. Burstein, D. L. Mills, A. Pinczuk, and S. Ushioda, Phys. Rev. Letters **22**, 348 (1969); E. Burstein and D. L. Mills, Phys. Rev. (to be published).

[12] S. V. Tyablikov, *Methods in the Quantum Theory of Ferromagnetism* (Plenum Publishing Corp., New York, 1967), Chap. IV.

where the $A^{\pm}$'s and $a^{\pm}$'s form column vectors of $2n$ positions. The total polariton Hamiltonian takes the form

$$\bar{H}=\sum_{\gamma \mathbf{k}} \omega(\mathbf{k}\gamma)A_{\mathbf{k}\gamma}{}^{+}A_{\mathbf{k}\gamma}{}^{-}. \tag{1.4}$$

This procedure, then, leads to a normal-mode Hamiltonian of familiar form, with polariton occupancy eigenstates of energy $\omega(\mathbf{k}\gamma)$.

Detailed solutions for the case of two and three levels coupling to light and interacting among themselves are given in Ref. 13. A special case of interest is that of light coupling to a series of n oscillators with coupling strengths $|g_i|^2 (i=1, \ldots, n)$ and neglecting the interaction between the oscillators. In this case, the eigenvalue equation becomes

$$\epsilon(\mathbf{k}\omega)\equiv \frac{k^2}{\omega^2}=1-4\sum_{i=1}^{n}\frac{|g_i|^2}{E_i(\mathbf{k})}\frac{1}{\omega^2-E_i{}^2(\mathbf{k})}. \tag{1.5}$$

The form of the polariton dispersion is illustrated in Fig. 1 for the special case of two levels coupled to light. The solid line represents the case $E(\mathbf{k})=E(0)$, while the dotted line is for $E(\mathbf{k})=E(0)+\frac{1}{2}\alpha k^2$.

In scattering theory,[14] if we call higher-order interactions V, one has the total Hamiltonian

$$H=\bar{H}+V \tag{1.6}$$

and the associated scattering operator

$$T_{\mathrm{pol}}(E)=V+V(E-H+i\epsilon)^{-1}V \tag{1.7}$$

describing the scattering of polaritons. Formally, one has the differential cross section for scattering from the state ψ to ψ' as[14]

$$\frac{d\sigma}{d\Omega}=\frac{2\pi}{v(\psi)}|\langle\psi|T_{\mathrm{pol}}(E)|\psi'\rangle|^2\rho_{\psi'}, \tag{1.8}$$

where v is the velocity function and ρ is the density of states.

When an external photon of energy E is incident on the crystal, then, in lowest order, polaritons of energy E are excited in the crystal. If only a single polariton satisfies the relation

$$\omega(\mathbf{k}\gamma)=E, \tag{1.9}$$

then the asymptotic polariton scattering state is defined uniquely by the label $(\mathbf{k},\gamma)$. If a number of polariton modes are degenerate at energy E, then one must determine the admixture of each mode excited in the crystal through the use of additional boundary conditions.

[13] B. Bendow, Ph.D. thesis, New York University, 1969 (unpublished).

[14] A. Messiah, *Quantum Mechanics* (John Wiley & Sons, New York, 1962), Vol. II, Chap. XIX.

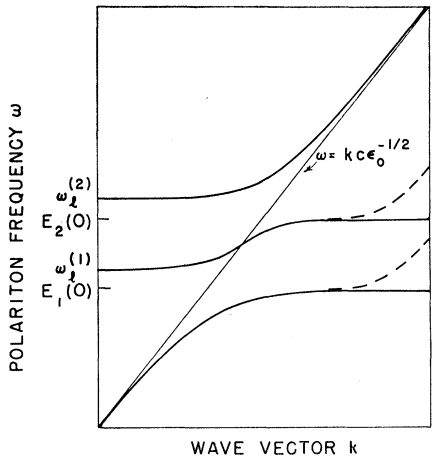

FIG. 1. Polariton frequency ω versus wave vector k for two bare-exciton levels coupling to light. The solid line is $E(k)=E(0)$ and the broken line is $E(k)=E(0)+\frac{1}{2}\alpha k^2$.

II. SINGLE AND MULTIBRANCH POLARITON CROSS SECTIONS

In the simplest case, both the initial and final polariton states are nondegenerate, and one obtains from Eq. (1.8), omitting damping effects entirely, the lowest-order contribution to $d\sigma/d\Omega$ as[2,11]

$$\frac{d\sigma}{d\Omega}=\frac{1}{(2\pi)^2}\frac{k'^2}{v_g(\mathbf{k}\gamma)v_g(\mathbf{k}'\gamma')}\times|\langle\mathbf{k}\gamma|V|\mathbf{k}'\gamma';[\mathbf{k}-\mathbf{k}']\rangle|^2, \tag{2.1}$$

where $[\mathbf{k}-\mathbf{k}']$ indicates occupancy of a phononlike polariton, and where we have used (neglecting the phonon dispersion)

$$v(\mathbf{k}\gamma)=\frac{\partial\omega(\mathbf{k}\gamma)}{\partial k}\equiv v_g(\mathbf{k}\gamma), \qquad \rho(\mathbf{k},\mathbf{k}')=(2\pi)^{-3}k'^2/[\partial\omega(\mathbf{k}'\gamma')/\partial k']. \tag{2.2}$$

The result for $d\sigma/d\Omega$ in this form is not entirely useful in the case of a polariton formed from a discrete nearly dispersionless level. As may be seen from Fig. 1, one then has a region in incoming photon energy in which no polariton state can be defined, and, consequently, the cross section is undefined; also, as $\omega\rightarrow E(0)$ from below, $v_g\rightarrow 0$, so that the cross section blows up. Hence, for this case, one must either introduce a version of polariton theory which includes damping and multipolariton effects, or else restrict one's self to the region outside of the "reflection zone."

For the case of insulators such as CdS, the dispersion of the exciton of the form

$$E(\mathbf{k})=E(0)+(2m^*)^{-1}k^2, \tag{2.3}$$

where m^* is the total electron-hole effective mass, enables one to define polariton states for all frequencies,

as may be seen from Fig. 1. In this paper, we discuss polariton scattering for such a case, without the explicit inclusion of damping effects.

The points in energy at which the various polariton branches intersect $k=0$ (for $\omega>0$) will be denoted by ω_l's. In the region below the lowest ω_l, one has single-branch polariton kinematics for Stokes RS, and the formula of Eq. (2.1) may be applied as stands, with $\gamma=\gamma'$.

Let us choose for V a trilinear exciton-phonon interaction of the form[9]

$$V=\sum_{\pm\mathbf{kq}} g(\pm\mathbf{kq})B_{\mathbf{k}+\mathbf{q}}{}^{+}B_{\mathbf{k}}{}^{-}b_{\mp\mathbf{q}}{}^{\pm}, \qquad (2.4)$$

where the B's are exciton and the b's phonon operators. The coupling function g is given explicitly for various cases in Ref. 9.

An analysis of $d\sigma/d\Omega$ for this case follows from an analysis of the behavior of two factors[13]: (a) the dynamical factor $k'^2/(v_y v_g')$ and (b) the matrix element of V [which we will denote by $V(\mathbf{k},\mathbf{k}')$].

The dynamical factor is a monotone-increasing function of ω as $\omega\rightarrow E(0)$ until the bend in the polariton curve near $E(0)$ is reached. The rapid increase in v_g immediately above $E(0)$ [cf. Fig. 2(a)] leads to a decrease in the dynamical factor for ω immediately above $E(0)$, followed by a return to monotone-increasing behavior for larger ω.

Assuming $g(\mathbf{k},\mathbf{k}')$ constant for the wave vectors of interest, the dependence of $V(\mathbf{k},\mathbf{k}')$ is contained nearly entirely in the transformation coefficients between polaritons and bare excitons. The transformation between the relevant phonon operators and polaritons for scattering of incident photon frequencies in the optical region may be taken to be nearly unity. The behavior of these coefficients as a function of frequency is illustrated in Fig. 2(b) and is seen to be strongly monotone increasing as $E(0)$ is approached, followed by saturation to unity above $E(0)$.

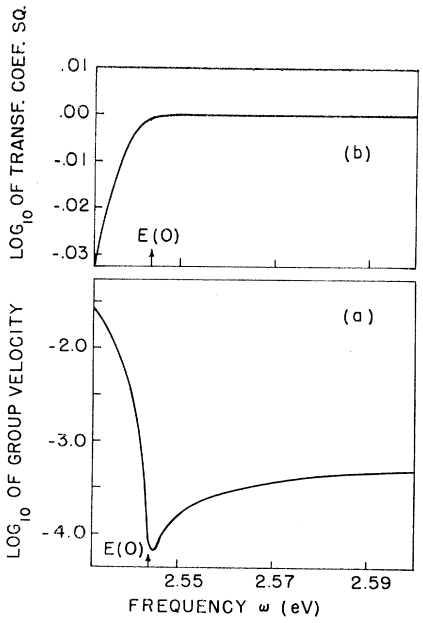

FIG. 2. Log_{10} of (a) group velocity and (b) square of the exciton-polariton transformation coefficient versus frequency ω, for CdS parameters: $E(0)=2.544$ eV, $|g|=0.2$ eV, $\alpha=(4.3\times10^5\ \mathrm{eV})^{-1}$.

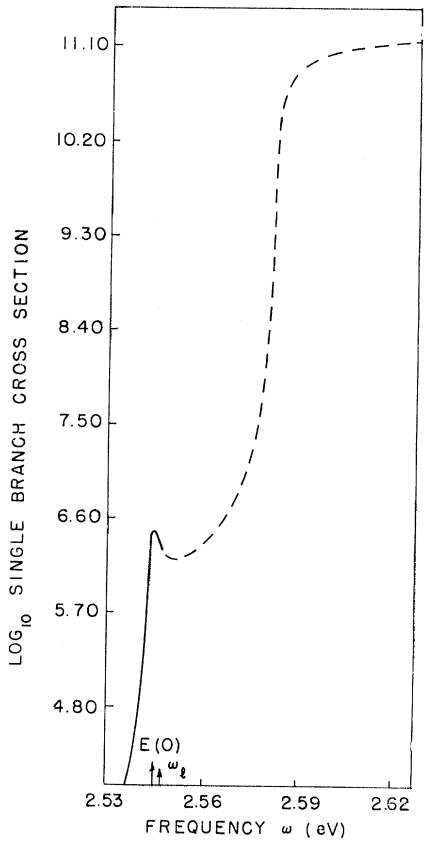

FIG. 3. Log_{10} of the single branch RS cross section in CdS. The broken line indicates the result in the region above ω where the single-branch result is not the total RS cross section.

The combined behavior of the dynamical factor and $V(\mathbf{k},\mathbf{k}')$ for parameters appropriate to CdS is illustrated in Fig. 3. One has strong enhancement coming into $E(0)$, followed by a small dip. The dotted-line portion refers to the same calculation extended to the region above ω, which is not a valid result for the total RS cross section in that region.

In the multibranch case, once the cross-section calculation is to be extended into regions of ω where either the in- or outgoing polariton is not unique (as is the case for $\omega>\omega_l$ in the dispersive case in Fig. 1), the simplified form for $d\sigma/d\Omega$ as given in Eq. (2.1) is no longer adequate. For example, the correct choice for the velocity function is no longer clear.

We will, therefore, generalize the definition of the

cross section, taking $d\sigma/d\Omega$ as

$$\frac{d\sigma}{d\Omega}=\tfrac{1}{2}(2\pi)^{-3}\sum_{\gamma\gamma'}\int\int d\mathbf{k}'dk\delta(E(\{\mathbf{k}\gamma\})-\omega)$$
$$\times\delta(E(\{\mathbf{k}',\gamma'\})-\omega')|\langle\{\mathbf{k}\gamma\}|T|\{\mathbf{k}'\gamma'\}\rangle|^2, \quad (2.5)$$

where $\{\mathbf{k},\gamma\}$ are the momentum and branch indices describing a polariton state. This generalization obeys the microreversibility requirement, and it reduces to Eq. (2.1) for the case where one has a single unique polariton at both ω and $\omega-\omega_0$, when one uses

$$\int d\mathbf{k}\delta[E(\mathbf{k}\gamma)-\omega]=\frac{4\pi k_0^2}{[\partial E(\mathbf{k}\gamma)/\partial k]_{k_0}}, \quad (2.6)$$

where $\mathbf{k}_0$ satisfies

$$E(\mathbf{k}_0,\gamma)=\omega. \quad (2.7)$$

When a number of polaritons are degenerate at the frequency ω, we will write the state $|\{\mathbf{k}\gamma\}\rangle$ as

$$|\{\mathbf{k}\gamma\}\rangle=\sum_{\mathbf{k}\gamma\gamma}\alpha(\mathbf{k}_\gamma\gamma)|\mathbf{k}_\gamma\gamma\rangle, \quad (2.8)$$

where the states $|\mathbf{k}_\gamma\gamma\rangle$ are polaritons of frequency ω, and where the coefficients α must be determined by additional boundary conditions.[15,16] An example of how such a procedure may be actually carried out is given in Sec. III. One then obtains, in the general case, neglecting phonon dispersion,

$$\frac{d\sigma}{d\Omega}=(2\pi)^{-2}\sum_{\gamma\gamma'}|\alpha(\mathbf{k}_\gamma\gamma)|^2|\alpha\mathbf{k}'(\gamma\gamma')|^2[k'(\gamma\gamma')]^2$$
$$\times[v_g(\mathbf{k}_\gamma\gamma)v_g\mathbf{k}'(\gamma\gamma')]^{-1}|\langle\mathbf{k}_\gamma\gamma|T|\mathbf{k}'\gamma,\gamma'\rangle|^2, \quad (2.9)$$

where $k'(\gamma\gamma')$ is the value of $k_{\gamma'}$ that satisfies the relation

$$\omega(\mathbf{k}_\gamma\gamma)=\omega(\mathbf{k}_{\gamma'}\gamma')+\omega_0. \quad (2.10)$$

This result is identical to the one which would be obtained if the scattering process was considered to consist of individual incoherent scatterings of all the allowed polaritons, and it is the form that will be employed for the calculations of the present paper. In fact, the results of Sec. III will show that, except for the region in energy immediately above $\omega+\omega_0$, a single scattering channel dominates the cross section in each of the various energy regions, so that, in any case, interference effects are expected to be small throughout most of the energy regions of interest.

III. CALCULATIONS FOR MODEL SYSTEM

In this section, we calculate the LO-phonon RS cross section due to the $n=1$ exciton of the A exciton in CdS, as an example of a two-branch polariton RS calculation.

[15] J. J. Hopfield and D. G. Thomas, Phys. Rev. **132**, 563 (1963).
[16] J. J. Sein, Ph.D. thesis, New York University, 1969 (unpublished).

The simplest application of the polariton RS theory developed in Sec. II is to a two-branched polariton system formed from the coupling of a photon to a single discrete exciton level. One may approximate the phonon-region polariton in the problem as being simply a phonon. Then the two-branch polariton illustrated in Fig. 4 contains all the necessary information describing the kinematics of the scattering.

One must determine the wave function expansion coefficients of Eq. (2.8); referring to the lower branch as 1 and the upper branch as 2, then, for $\omega<\omega_l$, one has $\alpha_1=1$, and $\alpha_2=0$, while α_1, $\alpha_2\neq0$ for $\omega>\omega_l$. For this region, we must introduce an additional boundary condition to determine α_1 and α_2.

We will assume, following the work of Ref. 16, that for this case the ratio of the squares of the classical electric fields associated with each polariton mode is proportional to the ratio of the probability amplitudes associated with each polariton, namely, $|\alpha_2/\alpha_1|^2$. For normal incidence, one may show that

$$\left|\frac{E_2}{E_1}\right|^2\equiv T(\omega)=\left|\frac{(n_1-1)+(n_1+1)r(\omega)}{(n_2-1)+(n_2+1)r(\omega)}\right|^2, \quad (3.1)$$

where the E's are electric field amplitudes, $n_i\equiv k_i/\omega$, and r is the ratio of the amplitude of the reflected wave to that of the incident. Using a boundary condition obtained through an extinction theorem for polariton waves, Ref. 16 has computed the reflectivity $R(\omega)\equiv|r(\omega)|^2$ and obtained good agreement with experimental data from Ref. 15. In our calculations, we, therefore, employ the theoretical formula for $r(\omega)$ in Ref. 16.

The reflectivity $R(\omega)$ and amplitude ratio $T(\omega)$ computed for parameters appropriate to CdS (but for

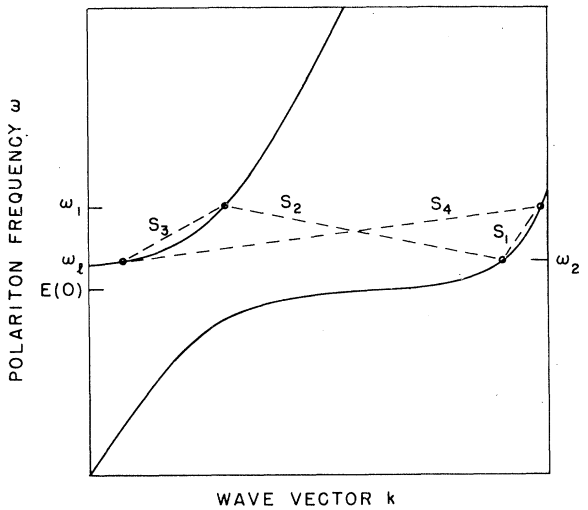

FIG. 4. Two-branched polariton dispersion curve versus wave vector for a single dispersive-exciton level coupled to light. The four possible scattering channels (s_i) corresponding to Stokes RS of a photon of energy ω_1 to a photon of energy ω_2, are indicated by broken lines.

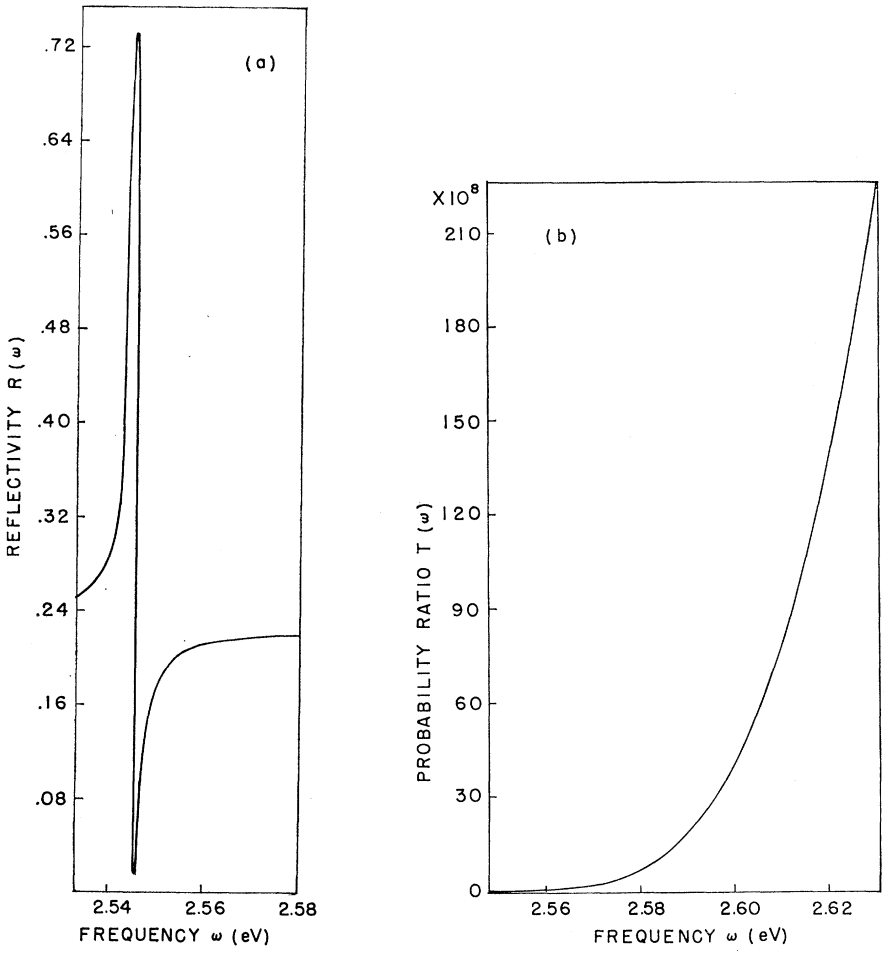

FIG. 5. (a) Reflectivity $R(\omega)$ and (b) probability ratio of upper-branch to lower-branch polariton $T(\omega)$ versus frequency ω, for CdS parameters (cf. Fig. 2).

zero damping) are illustrated in Fig. 5. Although it is necessary to include a finite damping to obtain the best fit to the observed $R(\omega)$, the results for $d\sigma/d\Omega$ are less sensitive to Γ, and for simplicity we, therefore, take $\Gamma=0$ in the calculation. As one notes from Fig. 6, in the region above ω_l, $T(\omega)$ increases rapidly, so that in this region, for the effective mass dispersion model, the upper-branch polariton strongly dominates the lower.

Figure 4 illustrates the maximum number of possible scattering channels, denoted by s_i, $i=1, \ldots, 4$. For $\omega<\omega_l$, just s_1 is open; for $\omega_l<\omega<\omega_l+\omega_0$, s_1 and s_2 are open; and for $\omega>\omega_l$, all four channels are open. In our approximation, the cross section is discontinuous at ω_l and $\omega_l+\omega_0$. One expects that the discontinuities would be smoothed out by inclusion of damping effects; the damping is certainly finite, although $\Gamma\ll|g|^2, E(0)$.

Figure 6 illustrates the dependence of the four separate RS cross sections from the four channels illustrated in Fig. 4, unmodulated by the α_i's in Eq. (2.9). Once the modulation by the α_i's has been included, the resulting contributions become those illustrated in Fig. 7. To obtain Fig. 7 we require the amplitudes $|\alpha_3|^2$ and $|\alpha_4|^2$. These were determined by employing transmittivities of the electric field portion of polaritons 3 and 4 at the boundary, analogously to Eq. (3.1). For $\omega<\omega_l$, s_1 is the dominant channel; for $\omega_l<\omega<\omega_l+\omega_0$, s_2 dominates; immediately above ω_l, both s_2 and s_3 contribute, s_3 eventually becoming the dominant channel. The total RS cross section for CdS, best-fitting points near the discontinuities, is illustrated in Fig. 8. One notes the double peaking associated with the in- and outgoing photon resonances, and the dominance of the higher-energy peak. These features are discussed and compared with other results in Sec. IV.

Figure 9 illustrates the dependence of $d\sigma/d\Omega$ on the photo-exciton coupling function g. While one obtains narrow Lorentzian-like peakings for small $|g|$, as $|g|^2\rightarrow E(0)\epsilon_0^{-1}$, one obtains wider, more asymmetrical peaks, and the discontinuity at $\omega_l+\omega_0$ becomes more pronounced.

The dependence of $d\sigma/d\Omega$ on the background dielectric constant ϵ_0 is illustrated in Fig. 10. For decreasing ϵ_0, one notes behavior similar to increasing $|g|$, as discussed above, except that the lower-energy peak decreases in height, while the higher-energy peak increases.

IV. LIMITING FORM OF $d\sigma/d\Omega$ FOR $\omega \ll E(0)$; CONTINUUM CONTRIBUTIONS

In this section, we discuss the limiting form of the cross section for ω far below $E(0)$, and the effect of the exciton continuum on the cross section below the energy gap E_g.

A. Limiting Form of $d\sigma/d\Omega$ for $\omega < E(0)$

For $\omega < E(0)$, one obtains, for the two-branch model of Sec. III,

$$\frac{d\sigma}{d\Omega} = \frac{(2\pi)^{-2}k'^2}{(\partial\omega/\partial k)(\partial\omega'/\partial k')} |V(\mathbf{k},\mathbf{k}')|^2 F(\mathbf{k}\omega) F(\mathbf{k}'\omega'),$$

$$F(\mathbf{k}\omega) \equiv \frac{|g|^2[\omega + E(\mathbf{k})]^2 \epsilon_0^{-1}}{\omega\{[\omega^2 - E^2(\mathbf{k})]^2 + 4|g|^2 E(\mathbf{k})\epsilon_0^{-1}\}}. \quad (4.1)$$

For ω, such that

$$\omega^2 - E^2(\mathbf{k}) \ll 4|g|^2 E(0)\epsilon_0^{-1}, \quad (4.2)$$

one has

$$\partial\omega/\partial k, \quad \partial\omega'/\partial k' \longrightarrow \epsilon_0^{-1/2}, \quad (4.3)$$

so that

$$d\sigma/d\Omega \cong (2\pi)^{-2}(k'/k)|g|^4 V(\mathbf{k},\mathbf{k}') \times [\omega - E(\mathbf{k})]^{-2}[\omega' - E(\mathbf{k}')]^{-2}. \quad (4.4)$$

However, this form is identical to that which arises in the bare-[9] or generalized-exciton[10] theories, when the condition of Eq. (4.2) is met, as long as $\Gamma \ll |g|$, which is the case for the insulators under study here. The region

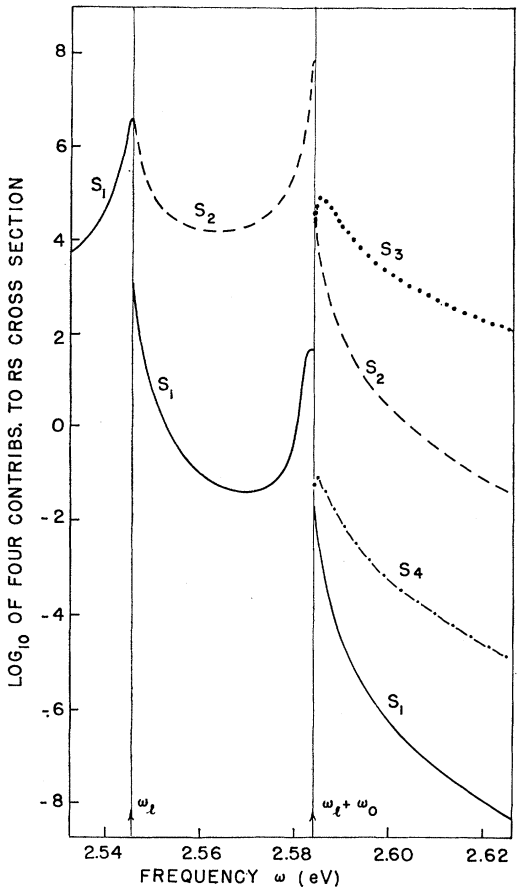

FIG. 7. Log_{10} of the four actual contributions to the RS cross section versus frequency ω, for CdS.

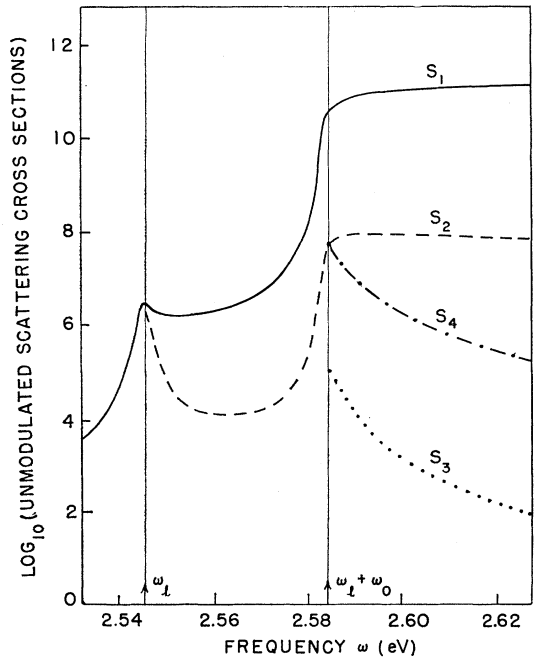

FIG. 6. Log_{10} of the four RS cross sections (arbitrary units) corresponding to the four channels of Fig. 4, unmodulated by the expansion coefficients α_i, versus frequency ω, for CdS parameters.

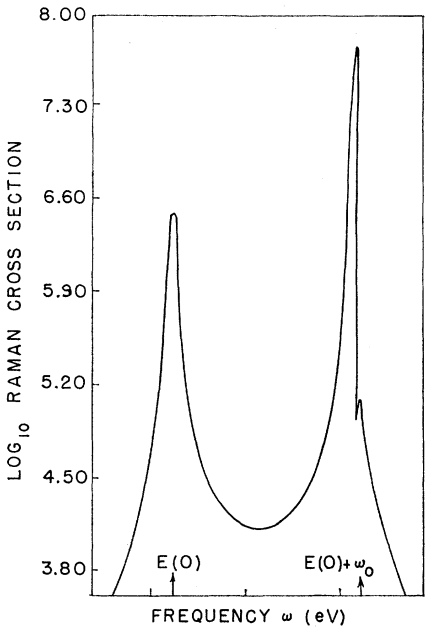

FIG. 8. Log_{10} of RS cross section (arbitrary units) versus frequency ω, for CdS. The curve is the best fit through the discontinuities at ω_l and $\omega_l + \omega_0$.

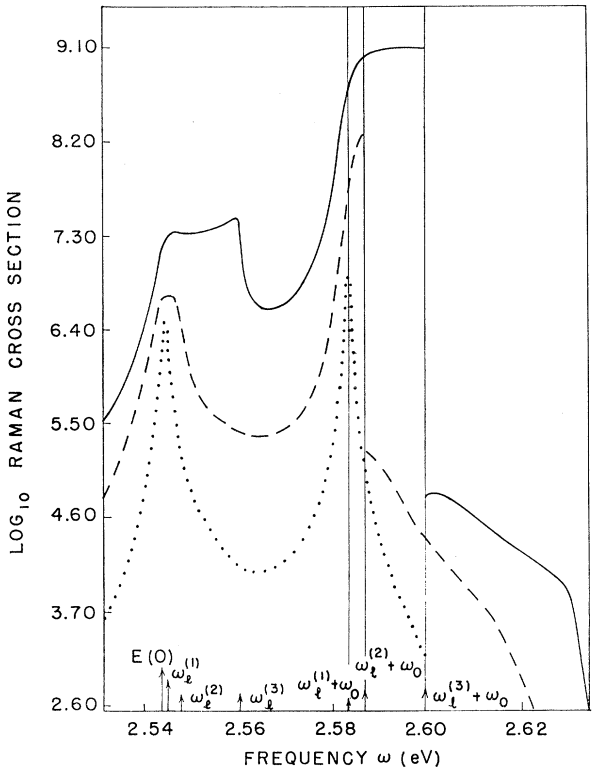

FIG. 9. Comparison of polariton-theory predictions for $\log_{10}$ of RS cross section versus frequency ω, for various values of photon-exciton coupling $|g|$. The solid line is $|g|=0.65$ eV, $\epsilon_0=8$; the dashed lines $|g|=0.4$ eV, $\epsilon_0=10$; and the dotted lines $|g|=0.2$ eV, $\epsilon_0=10$, $m^*=0.85\ m_e$, $E(0)=2.544$ eV for all cases.

in ω satisfying Eq. (4.2) will be referred to as a photonic region (photon-polariton transformation coefficient nearly unity).

B. Contribution of Exciton Continuum

Before comparison with experiment, one must consider the contribution of the exciton continuum to the RS cross section.[17] Strictly speaking, a rigorous polariton theory of continuum effects necessitates the enlargement of the matrices D and G of Eq. (1.2) to include a continuous index allowing the incorporation of the continuum. We do not here treat the discrete-continuum polariton problem in this way; rather, we discuss the continuum contribution to RS1 in the frequency region below the gap E_g by a version of perturbation theory, which we now describe.

We write the scattering operator T as

$$T=V+V_{CR}+(V+V_{CR})(E-H+i\epsilon)^{-1}(V+V_{CR}), \quad (4.5)$$

$$H=\bar{H}+H_C+V+V_{CR},$$

where $\bar{H}$ and V are the previously employed operators referring to discrete excitons and polaritons, except that V is now understood to include interactions with continuum excitons also; H_C is the free-field continuum exciton Hamiltonian

$$H_C=\sum_{\mathbf{k}\eta}\omega(\mathbf{k}\eta)B_{\mathbf{k}}^{+}(\boldsymbol{\eta})B_{\mathbf{k}}^{-}(\boldsymbol{\eta}), \quad (4.6)$$

where

$$\omega(\mathbf{k}\eta)=E_g+(2m^*)^{-1}k^2+(2\mu)^{-1}\eta^2, \quad (4.7)$$

where $\boldsymbol{\eta}$ is the electron-hole relative motion wave vector and μ is the electron-hole reduced mass. V_{CR} is the continuum-exciton-photon bilinear interaction, of the form ($a^{\pm}$'s denote photon operators)

$$V_{CR}=\sum_{\mathbf{k}\eta\pm}g_{CR}(\pm\pm\mathbf{k}\eta)a_{\mathbf{k}}^{\pm}B_{\mathbf{k}}^{\pm}(\boldsymbol{\eta}). \quad (4.8)$$

In T, let us use the expansion

$$G=G_1+G_1(V+V_{CR})G_1+\cdots, \quad (4.9)$$

where

$$G\equiv(E-H+i\epsilon)^{-1}, \quad G_1\equiv(E-\bar{H}-H_C+i\epsilon)^{-1}. \quad (4.10)$$

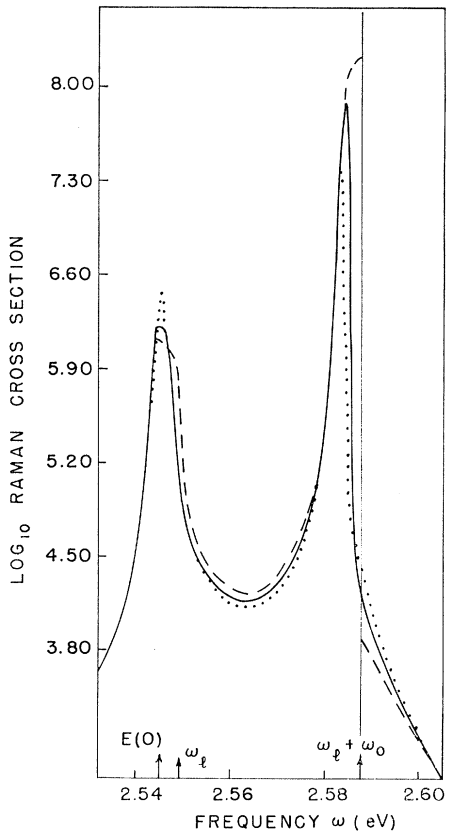

FIG. 10. Comparison of polariton-theory predictions of $\log_{10}$ of RS cross sections versus frequency ω, for various values of background dielectric constant ϵ_0. The solid line is $\epsilon_0=4$; the dashed line is $\epsilon_0=2$; and the dotted line is $\epsilon_0=8$. $|g|=0.2$ and $m^*=0.85\ m_e$, $E(0)=2.544$ eV, for all cases.

[17] B. Bendow, J. L. Birman, A. K. Ganguly, T. C. Damen, R. C. C. Leite, and J. F. Scott, Optics Comm. 1, 267 (1970).

Let us denote continuum-exciton occupancy by use of $\boldsymbol{\eta}$'s. Now for $\omega<E_g$, in a region where a single unique polariton exists for both ω and ω', one has the transition matrix element for RS1 as

$$\langle \mathbf{k}\gamma|\, T\,|\mathbf{k}'\gamma', [\mathbf{k}-\mathbf{k}']\rangle \cong T_1+T_2+T_3,$$

$$T_1=\langle \mathbf{k}\gamma|\, V\,|\mathbf{k}'\gamma', [\mathbf{k}-\mathbf{k}']\rangle,$$

$$T_2=\sum_{\eta}\{\langle \mathbf{k}\gamma|\, V_{CR}|\mathbf{k}\boldsymbol{\eta}\rangle[\omega-\omega(\mathbf{k}\boldsymbol{\eta})]^{-1} \times\langle \mathbf{k}\boldsymbol{\eta}|\, V\,|\mathbf{k}'\gamma', [\mathbf{k}-\mathbf{k}']\rangle+(V\rightleftarrows V_{CR}, k\rightleftarrows k')\},$$

$$T_3=\sum_{\eta\eta'}[\langle \mathbf{k}\gamma|\, V_{CR}|\mathbf{k}\boldsymbol{\eta}\rangle[\omega-\omega(\mathbf{k}\boldsymbol{\eta})]^{-1} \times\langle \mathbf{k}\boldsymbol{\eta}|\, V\,|\mathbf{k}'\boldsymbol{\eta}', [\mathbf{k}-\mathbf{k}']\rangle[\omega-\omega(\mathbf{k}'\boldsymbol{\eta}')]^{-1} \times\langle \mathbf{k}'\boldsymbol{\eta}'|\, V_{CR}|\mathbf{k}'\gamma'\rangle\}. \quad (4.11)$$

T_1 is the discrete polariton contribution as employed previously, while T_2 and T_3 are continuum effects. To investigate their contributions, one notes that

$$\langle \mathbf{k}\gamma|\, V_{CR}|\mathbf{k}\boldsymbol{\eta}\rangle=c_1(\mathbf{k}\gamma)g(\mathbf{k}\boldsymbol{\eta}), \quad (4.12)$$

where $c_1(\mathbf{k}\gamma)$ is the transformation coefficient between a photon and polariton, which is nearly unity in the photonic region; for $\omega\rightarrow E(0)$, $c_1(\mathbf{k}\gamma)$ decreases to nearly zero. Then one sees that T_3 is identical to the continuum contribution obtained in bare-exciton theory (if the bilinear phonon-exciton interaction is omitted), in the photonic region. T_2 is a purely polariton term with no lowest-order bare-exciton analog.

Let us employ the approximations listed in Ref. 9 for q_e and q_h (the electron-hole wave function modulation of the trilinear coupling functions)

$$q_e,\, q_h\approx\delta_{\lambda\lambda'} \quad \text{for} \quad \mathbf{k}-\mathbf{k}'\approx 0, \quad (4.13)$$

where the λ's are intrabranch exciton indices, discrete or continuous; then the T_2 contribution vanishes.

V. DISCUSSION AND COMPARISON WITH OTHER RESULTS AND WITH EXPERIMENT

In this section, we compare the results of the present paper with those of the bare- and generalized-exciton approaches, and with available experimental data.

As discussed in Sec. IV, for the case of a single discrete exciton level $E(0)$, one obtains, in the photonic region below $E(0)$, the same result for $d\sigma/d\Omega$ from both the exciton and polariton approaches.

Regarding the continuum contributions in polariton theory, within the approximations of Sec. IV, these are identical to the bare-exciton contribution in the photonic region. As $\omega\rightarrow E(0)$, $T_3\rightarrow c_1(\mathbf{k}\gamma)c_1(\mathbf{k}'\gamma')\times$(bare-exciton contribution), with c_1 the photon-polariton transformation coefficient (cf. Sec. IV), so that in this region the polariton contribution is smaller than the bare exciton one. However, the bare-exciton calculation described in Ref. 17 demonstrates that, as $\omega\rightarrow E(0)$, the discrete exciton contribution substantially outweighs the continuum contribution, even for values of ω still within the photonic region. Consequently, the difference in the contributions of the two theories in the region near $E(0)$ has very little effect on the total RS cross section.

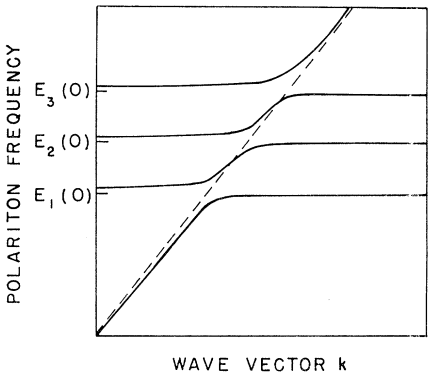

FIG. 11. Polariton dispersion versus wave vector for the small coupling case.

These arguments may be extended to deal with the entire region in ω below E_g. For the small coupling case (cf. Fig. 11) one has successive regions where a polariton branch is nearly parallel to the photon line $\omega=kc\epsilon_0^{-1/2}$. In these photonic regions, the bare exciton and polariton contributions to T_3 are nearly equal. In the regions of the splittings, the discrete exciton terms dominate $d\sigma/d\Omega$, and one need not include the continuum contributions in the calculation. For larger couplings, one has larger regions of splitting in which, again, discrete exciton effects dominate.

One may then conclude that for $E<E_g$, and within the approximations employed, the effect of the exciton continuum on the total RS cross section is nearly the same for the polariton as well as for the bare- and generalized-exciton approaches. For this reason, we will, in what follows, compare only the discrete exciton contributions of the various theories.

As shown in Ref. 10, bare-exciton theory and generalized-exciton theory yield nearly identical results, for small couplings satisfying $\epsilon_0|g|^2/4E(0)\lesssim 0.035$. As was done there, an *ad hoc* damping term will be employed for the bare theory and assumed identical to the trilinear damping interactions in the generalized theory. The values of damping employed for CdS are of the order of magnitude of these employed by Ref. 16 to obtain a fit to observed CdS reflectivity data.

Figure 12 (a) illustrates the comparison between the bare-exciton and polariton (cf. Sec. III) approaches for small coupling (CdS parameters). The two results are very similar, especially on the low-energy side; however, the high-energy polariton peak does dominate the exciton one. The results of the three approaches

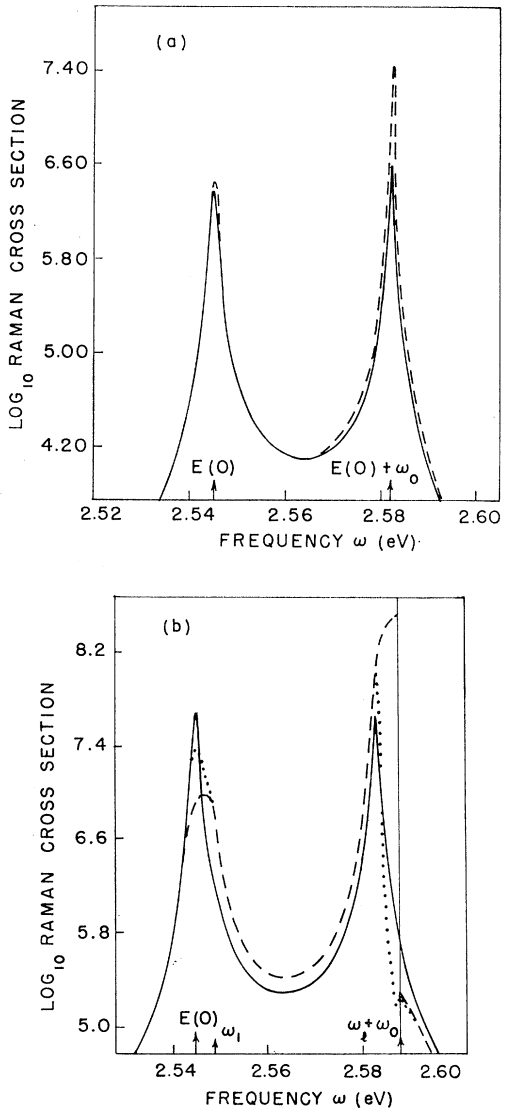

FIG. 12. Comparison of polariton- and exciton-theory predictions for $\log_{10}$ of RS cross section versus frequency ω. (a) Small coupling CdS parameters as given in Fig. 2. The solid line is the bare- and generalized-exciton result and the dashed line is the polariton result. (b) Large coupling, $|g|=0.5$ eV, other parameters as in Fig. 2. The solid line is the bare exciton result, the dashed line is the polariton result and the dotted line is the generalized exciton result. The exciton theories have employed damping $\Gamma=6\times10^{-4}$ eV.

for larger coupling are illustrated in Fig. 12(b). While the bare-exciton peaks are symmetrical regardless of $|g|$, the higher- dominates the lower-energy peak for both the polariton and generalized exciton results. One notes the agreement between the various theories for all cases in a region below $E(0)$, as discussed in detail in Sec. IV.

We now consider the comparison between theory and experiment. References 8 and 17 show that good agreement is obtained between the observed enhancement and the predictions of bare-exciton theory, for LO phonon RS in CdS, as $\omega \rightarrow E(0)$. As such, the nearly identical prediction of polariton theory in this region also agrees with experiment. Unfortunately, sufficient data on the dependence on incoming photon frequency between $E(0)$ and $E(0)+\omega_0$ is not presently available. However, the appearance of the outgoing photon resonance in Nth order RS $[\omega \cong E(0)+N\omega_0$, or $\omega' \cong E(0)]$ has been observed,[18] so that a double peaking associated with in- and outgoing resonances is in agreement with experiment. Further discussion of the comparison between bare-exciton theory and the experiments mentioned here is given in Refs. 17 and 18.

As may be inferred from Fig. 12(b), the most marked differences between the various theoretical predictions occur for larger couplings, so that experiments in such materials would aid in evaluating the relative merits of the various approaches. Even for weak couplings, however, experimental data in the immediate region of the two peaks would be highly useful, in view of the different predictions as to the relative height of the two peaks.

In conclusion, we point out two ways in which the considerations of this paper might be generalized. First, we have omitted damping entirely in the asymptotic polariton scattering states and the associated group velocities; the theory needs to be extended to include the effects of small but finite dampings. Second, further examination of the explicit form of the coupling functions, and their frequency dependence, is necessary. Such a program would, in general, require the investigation of the microscopic interaction mechanisms leading to the couplings. As an example of the necessity for such investigations, we note that although the simplified forms for the coupling as employed here and in Refs. 9 and 10, e.g., have successfully accounted for various features of the observed LO RS in CdS, they apparently cannot account for certain features of the observed TO scattering.[8]

[18] R. C. C. Leite, J. F. Scott, and T. C. Damen, Phys. Rev. Letters 22, 780 (1969).